Elastocaloric and magnetocaloric effects in Ni-Mn-Sn(Cu) shape-memory alloy

Pedro O. Castillo-Villa, Lluís Mañosa, Antoni Planes, Daniel E. Soto-Parra, J. L. Sánchez-Llamazares, H. Flores-Zúñiga, and Carlos Frontera

Citation: Journal of Applied Physics **113**, 053506 (2013);

View online: https://doi.org/10.1063/1.4790140

View Table of Contents: http://aip.scitation.org/toc/jap/113/5

Published by the American Institute of Physics

Elastocaloric and magnetocaloric effects in Ni-Mn-Sn(Cu) shape-memory alloy

Pedro O. Castillo-Villa,[1] Lluís Mañosa,[1] Antoni Planes,[1] Daniel E. Soto-Parra,[2] J. L. Sánchez-Llamazares,[2] H. Flores-Zúñiga,[2] and Carlos Frontera[3]
[1]*Departament d'Estructura i Constituents de la Matèria, Facultat de Física, Universitat de Barcelona, Diagonal 647, E-08028 Barcelona, Catalonia*
[2]*Instituto Potosino de Investigación Científica y Tecnológica, Camino a la Presa San José 2055, Col. Lomas 4a, CP,78216. San Luis Potosí, México*
[3]*Institut de Ciència de Materials de Barcelona, Campus UAB, 08193 Bellaterra, Catalonia*

(Received 5 December 2012; accepted 16 January 2013; published online 5 February 2013)

We have studied magnetocaloric and elastocaloric properties of a Ni-Mn-Sn(Cu) metamagnetic shape-memory alloy undergoing a magneto-structural transition (martensitic type) close to room temperature. Changes of entropy have been induced by isothermally applying both mechanical (uniaxial stress) and magnetic fields. These entropy changes have been, respectively, estimated from dilatometric measurements giving the length of the sample as a function of temperature at selected applied forces and magnetic fields and from magnetization measurements as a function of temperature at selected applied magnetic fields. Our results indicate that the elastocaloric effect is conventional and occurs in two steps which reflect the interplay between the martensitic and the incipient magnetic transitions. By contrast, the magnetocaloric effect is inverse and occurs in a single step that encompasses the effect arising from both transitions. © *2013 American Institute of Physics*. [http://dx.doi.org/10.1063/1.4790140]

I. INTRODUCTION

Ferromagnetic shape-memory alloys (FSMAs) have attracted a lot of interest these last years due to their multifunctional behaviour which includes giant magnetostriction,[1–3] magnetoresistance,[4] and magnetocaloric effects.[5] These multiple functionalities rely on the possibility of both mechanically and magnetically inducing large changes in structural and magnetic properties which are strongly coupled to one another. This behaviour makes these materials potentially useful in diverse technologically interesting applications ranging from sensors and actuators to solid-state refrigerants.

In the present paper, we focus on the caloric properties of a Ni-Mn-Sn(Cu) alloy. This material belongs to the family of NiMn-based metamagnetic Heusler shape-memory compounds. At an appropriate composition, with excess of Mn with respect to the 2-1-1 stoichiometry, they undergo a martensitic transition below the Curie temperature within the ferromagnetic state. In the vicinity of this martensitic transition, these alloys display giant inverse magnetocaloric effect (IMCE) which means that a huge increase of entropy can be induced by isothermal application of a magnetic field, whereas cooling (decrease of temperature) occurs when the field is adiabatically applied.[6,7] This peculiar behaviour is related to the fact that an applied magnetic field favours the stabilization of the high temperature parent phase which has a higher magnetization than the martensitic phase. In addition to these interesting magnetocaloric properties, NiMn-based alloys also display mechanocaloric effects. In this case, changes of entropy or temperature can be induced by changing a mechanical field (or stress) isothermally or adiabatically, respectively. The barocaloric effect is a particular mechanocaloric effect induced by the application of hydrostatic pressure.[8–10] When it is induced by a uniaxial stress, it is commonly denoted as elastocaloric effect.[11] Recently, a large barocaloric effect has been reported to occur in the metamagnetic Ni-Mn-In shape-memory alloy.[9] This effect is a consequence of the relatively large volume-change taking place at the martensitic transition in metamagnetic shape-memory alloys.[5] Moreover, since the transition can be induced by application of a uniaxial stress, it is also expected that these materials also show elastocaloric effect.[11,12]

Addition of small quantities of a fourth element in the ternary Heusler alloys has been proposed in order to tailor transition temperatures and reduce the degree of hysteresis associated with the martensitic transition which is the main drawback for an efficient magnetocaloric effect to occur in metamagnetic shape-memory alloys. Cu, for instance, has been shown to have an important effect on the properties of the Ni-Mn-Sn compound. It has been reported that replacement of Mn by a little amount of Cu ($\leq 3\%$) in $Ni_{43}Mn_{46-x}Cu_xSn_{11}$ results in a considerable shift of the martensitic transition to a higher temperature[13] while the transition slightly shifts to a lower temperature when Cu replaces Ni in $Ni_{46-x}Cu_yMn_{43}Sn_{11}$.[14] In the present paper we study elastocaloric and magnetocaloric properties in a highly Cu-doped Ni-Mn-Sn. As far as we are aware, this is the first combined study of these two caloric effects in a metamagnetic shape-memory material.

The paper is organized as follows. In Sec. II, experimental details, sample characteristics, and methods are described. The obtained experimental results are presented in Sec. III. Finally, in Sec. IV, the obtained results are briefly discussed and the main conclusions are summarized.

II. EXPERIMENTAL DETAILS AND SAMPLE CHARACTERIZATION

A polycrystalline $Ni_{43}Mn_{40}Sn_{10}Cu_7$ alloy was elaborated from pure elements by arc melting in Ar atmosphere. The ingot was encapsulated under vacuum in quartz glass, annealed at 1123 K (850 °C) during 24 h and quenched into an ice-water mixture. A specimen of size $4.6 \times 3.2 \times 3$ mm^3 (mass, $m \simeq 0.35$ g) for length change and calorimetric measurements was cut from the ingot by means of a low speed diamond saw. The length change was measured along the long dimension of the specimen. In the free state, at room temperature, the reference length is $L_0 = 4.6$ mm. A smaller specimen of mass 32.6 mg was cut from the same ingot for magnetic measurements. Transition temperatures were determined by means of DSC (TA Q2000, TA-Instruments) measurements. It was found that the studied alloy undergoes a martensitic transition on cooling starting at $M_S = 322 \pm 1$ K and finishing at $M_F = 317 \pm 1$ K; on heating the reverse transition starts at $A_S = 329 \pm 1$ K and finishes at $A_F = 336 \pm 1$ K (in the absence of applied mechanical and magnetic fields).

Magnetic measurements were carried out in a PPMS (Quantum Design) magnetometer. In Fig. 1(a), we show low field (50 Oe) magnetization measurements performed during cooling and heating runs. The obtained values of magnetization are low and reflect the paramagnetic character of the system. The sharp decrease of the magnetization on cooling and the corresponding increase on heating indicate the occurrence of the martensitic transition with associated relatively weak hysteresis of about 13 ± 1 K. It is worth pointing out that the lower value of the magnetization in the martensitic phase is a common feature of metamagnetic shape-memory Heusler alloys.[5]

Fig. 1(b) shows calorimetric measurements performed during heating and cooling runs. The hysteresis loop gives the fraction y of parent phase as a function of temperature T. At each temperature y was computed from de calorimetric curves giving the heat flow as a function of temperature (the one corresponding to the depicted loop is shown in the inset of Fig. 1(b)). For cooling runs, it is obtained as:

$$y(T) = 1 - \frac{1}{|\Delta S|}\int_{M_S}^{T} \frac{\dot{q}}{|\dot{T}|}\frac{dT}{T}, \tag{1}$$

and for heating runs as:

$$y(T) = \frac{1}{|\Delta S|}\int_{A_S}^{T} \frac{\dot{q}}{|\dot{T}|}\frac{dT}{T}. \tag{2}$$

$\dot{q}$ is the heat flow and $\dot{T}$ is the corresponding temperature rate. The integrals were numerically performed from M_S on cooling and from A_S on heating to a given temperature T within the transformation interval after choosing a suitable base line. ΔS is the transition entropy change corresponding to the complete transition. We have obtained $\Delta S = 54 \pm 1$ J/kg K. Note that the hysteresis loop obtained from calorimetric measurements is in good agreement with the corresponding one from magnetic measurements. The inset in Fig. 1(a) shows in detail the region of the calorimetric curves where the heat flow starts to deviate from the base line in the cooling (bottom) and heating (top) runs. The small feature indicated by arrows in the curves corresponds to the onset of the paramagnetic-ferromagnetic transitions at $T_{C_{A-M}} = 323 \pm 0.5$ K in the cooling run. The magnetic transition is not completed due to the simultaneous occurrence of the structural change associated with the martensitic transition. On heating, the magnetic transition is also detected at the onset of the reverse martensitic transition at $T_{C_{M-A}} = 333 \pm 0.5$ K. The existence of hysteresis in the magnetic transition indicates that this transition does not occur independently of the martensitic transition.

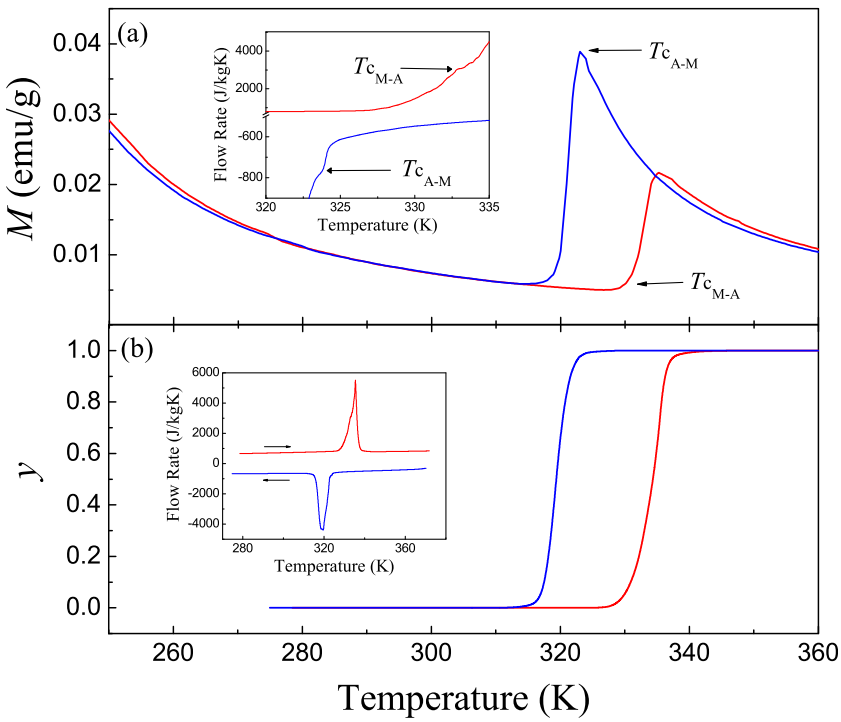

FIG. 1. (a) Low-field magnetization as a function of temperature under an applied magnetic field $H = 50$ Oe. (b) Martensitic transformed fraction y as a function of temperature obtained from calorimetric measurements (see text). A typical calorimetric run, at zero applied magnetic field, is shown in the inset of panel (b). The inset in panel (a) shows an enlargement of the calorimetric curves displayed in the inset of panel (b) in the regions of the beginning of the forward and reverse martensitic transitions. The small features indicated by arrows correspond to the magnetic transitions on cooling and heating.

The experimental procedure used to measure length change versus temperature under applied compression stress and magnetic field was reported in a previous work.[15] It consists of a temperature controlled sample holder placed between two cylindrical rods. The upper rod is in direct contact with the upper surface of the sample which is located between the poles of an electromagnet that enables application of magnetic fields up to 1 T. Compressive forces can be applied (perpendicular to the applied magnetic field) by increasing a weight put on the top end of the upper rod. The load is measured by a load cell located at the bottom end of the lower rod. The length changes are detected by means of a capacitive strain gauge attached to the upper rod.

III. MECHANIC AND MAGNETIC FIELD INDUCED ENTROPY CHANGES

In all experiments, the martensitic transition has been thermally induced (in order to ensure that it is completed) at selected values of the applied magnetic field $\mu_0 H$ and compression force F, which are kept constant in each run. From the curves giving the length L of the specimen as a function of temperature, entropy changes (per unit mass) induced by isothermally increasing the compression stress from 0 to σ can be computed from the general expression:

$$\Delta S(T,H,0\rightarrow\sigma)=\rho_0^{-1}\int_0^{\sigma}\left(\frac{\partial\varepsilon(T,\sigma,H)}{\partial T}\right)_{\sigma}d\sigma, \qquad (3)$$

where the Maxwell relation $(\partial S/\partial\sigma)_T=(\partial\varepsilon/\partial T)_\sigma$ has been taken into account. ρ_0 is the mass density. Taking into account that $\sigma=F/\phi$, with ϕ being the cross section of the specimen, and $\varepsilon=(L-L_0)/L_0$, we obtain that the stress- (or force-) induced entropy change corresponding to a change of the force from 0 to $F=\sigma\phi$ can be obtained as:

$$\Delta S(T,H,0\rightarrow F)=m_0^{-1}\int_0^{F}\left(\frac{\partial L(T,F,H)}{\partial T}\right)_{F}dF, \qquad (4)$$

where $m_0=\rho_0\Omega_0$, with $\Omega_0=\phi L_0$ being the corresponding reference volume of the specimen. Since the applied forces in our experiments are small, we assume that the cross section ϕ is constant.

In Fig. 2, as an example, we present the length of the specimen as a function of temperature for selected values of the applied stress and zero magnetic field during heating runs from below to above the martensitic transition. Prior to each of these experiments the specimen was first heated well above the transition and cooled down (at zero-stress) to a low enough temperature to ensure that the martensitic transition is completed. It is interesting to note that no anomaly in the length versus temperature curve is detected for very low applied forces. This is due to the self-accommodating microstructure of the thermally induced martensite. By increasing the force, two steps develop at about 332 K and 336 K. The low temperature step occurs precisely at onset of the magnetic transition on heating. By increasing the applied force, both steps have a tendency to shift to higher temperatures. This is shown in panel (f) of Fig. 2 where the derivative dL/dT has been plotted as a function of temperature for the $L(T)$ measurements depicted in panels (a) to (e). The inset of panel (e) gives the dependence of the maxima of dL/dT on

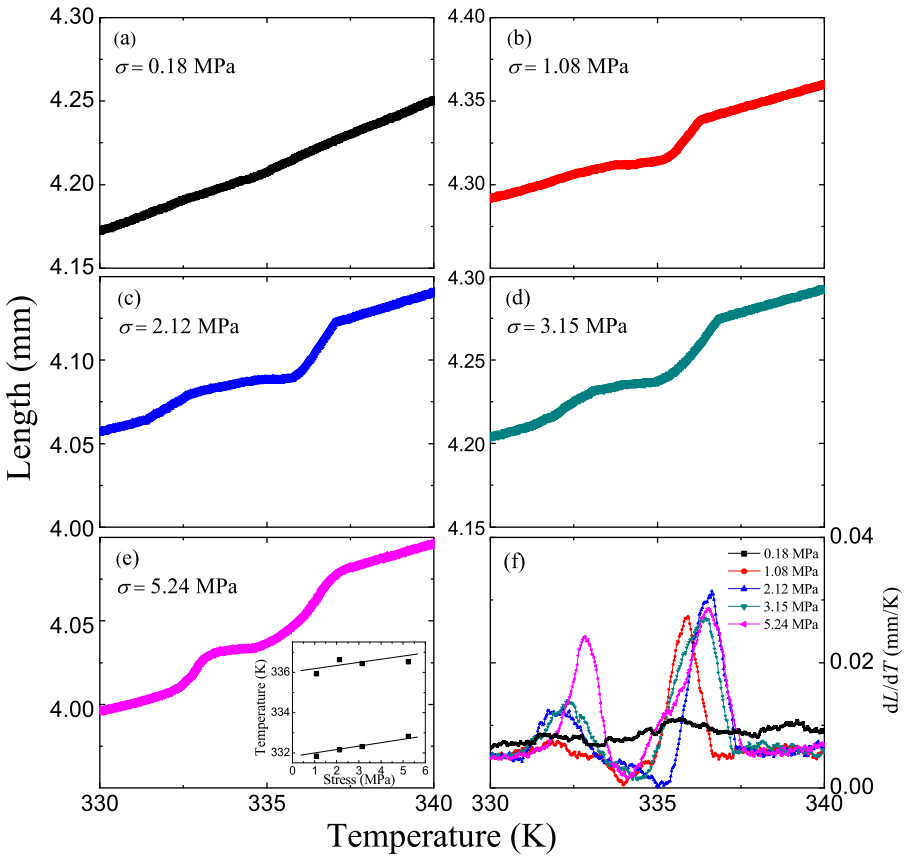

FIG. 2. Length of the sample as a function of temperature. Panels (a) to (e) correspond to increasing values of the stress from 0.18 MPa up to 5.24 MPa. Panel (f) shows the derivative dL/dT of the previous curves as a function of temperature. The inset in panel (e) shows the corresponding temperature of the maxima *vs.* the applied stress.

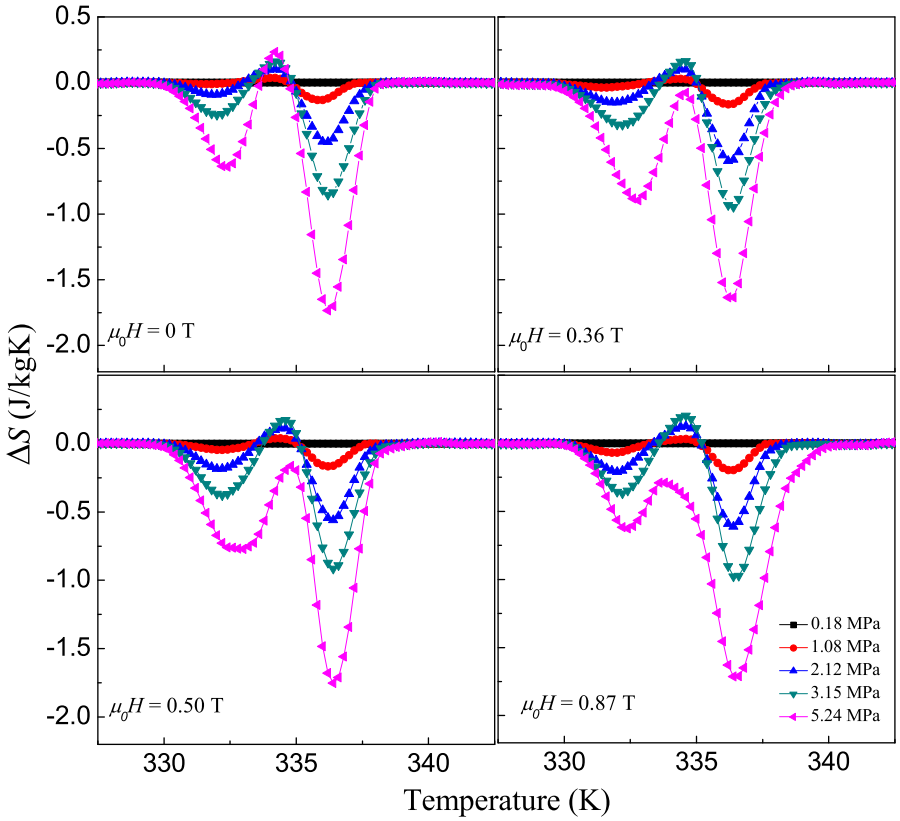

FIG. 3. Stress-induced entropy change as a function of temperature at selected values of an applied stress. The panels correspond to selected values of an applied magnetic field (indicated in each panel).

the applied stress. Both increase with the stress at a rate of ~0.2 K/MPa. This behaviour confirms that the magnetic transition on heating can only occur when the systems has started to retransform to the parent phase thus confirming the magneto-structural character of the magnetic transition which is triggered by the martensitic transition.

The isothermally stress-induced entropy changes derived from these curves are shown in Fig. 3 for selected values of applied magnetic field up to 1 T. At zero applied magnetic field, two peaks occur close to 332 K and 336 K. The effect of the applied magnetic field is remarkable. By increasing the field, the two peaks show a tendency to overlap. This effect can be understood taking into account, on the one hand, that for metamagnetic shape-memory alloys, it is expected that an applied magnetic field favours the stability of the parent phase and, on the other hand, the tendency of the magnetic field is to smear the magnetic transition.

Magnetic field induced entropy changes at zero stress have been obtained from the magnetization versus temperature curves measured at selected values of applied magnetic fields in the range from 0 to 5 T. Results are shown in Fig. 4. On heating a sharp increase of the magnetization occurs at the martensitic transition. The lower value of the magnetization in the martensitic phase must be a consequence of the enhancement of antiferromagnetic correlations as has been established in Ni-Mn-Sn from polarized neutron diffraction.[16] Actually, in the studied class of alloys, magnetic moments can be assumed to be localized at Mn-atoms to a very good approximation. These moments interact through an oscillatory RKKY-type exchange coupling (driven by conduction electrons), which bring the magnetic properties of these systems to be extremely sensitive to small variations of the distances between Mn-atoms. Within this scenario, it has been shown that antiferromagnetism arises from the excess of Mn-atoms with respect to the 2-1-1 stoichiometry that enables nearest neighbor Mn-Mn-pairs to exist in the martenitic phase that couple antiferromagnetically.[17,18] Consistently, in our case, the sharp step in the magnetization associated with the martensitic transition slightly shifts to lower temperatures by increasing the applied field. This result confirms the increase of the stability range of the parent phase under an applied magnetic field.

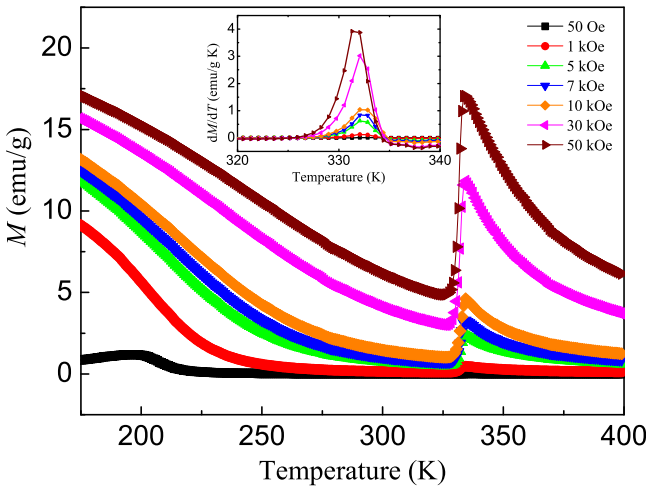

FIG. 4. Magnetization versus temperature curves at selected values of the applied magnetic field up to 50 kOe. The inset shows, for each magnetization curve, the derivative dM/dT as a function of the temperature in the region of the magneto-structural transition.

Magnetic field induced entropy changes (per unit mass) in the absence of applied stress have been obtained from the general thermodynamic expression,

$$\Delta S(T, 0 \rightarrow H) = \frac{\mu_0}{\rho_0} \int_0^H \left(\frac{\partial M(T,H)}{\partial T} \right)_H dH, \qquad (5)$$

where μ_0 is the magnetic permeability of free space. The obtained results are shown in Fig. 5. The magnetic field-induced entropy change as a function of temperature shows a single positive peak centered about 332 K, which corresponds to the low temperature peak in the stress induced entropy change versus temperature curves displayed in Fig. 3. This is consistent with the effect of an applied magnetic field on the stress induced entropy change previously discussed. In the present case, however, application of a magnetic field results in an increase of entropy while application of stress results in an entropy decrease. This means that while the elastocaloric effect in the studied materials is conventional, the magnetocaloric effect is inverse as expected for a metamagnetic shape-memory material.[5]

IV. DISCUSSION AND CONCLUSIONS

In this paper, we have studied elastocaloric and magnetocaloric properties of a highly Cu-doped $Ni_{43}Mn_{40}Sn_{10}Cu_7$ shape-memory alloy in the region of its martensitic transition. Both, above and below the martensitic transition, the system is paramagnetic. Incipient paramagnetic to ferromagnetic transitions occur at the onset of both forward and reverse martensitic transitions. These magnetic transitions are inhibited as the martensitic transition proceeds. The paramagnetic character of the materials above and below the martensitic transition is well demonstrated by the linear temperature dependence of the inverse susceptibility, shown in Fig. 6. From these curves, linear extrapolation to zero of the inverse-susceptibility enables to determine paramagnetic Curie temperatures for both phases. We have obtained $\theta_P = 311 \pm 2$ K, for the parent phase, and $\theta_M = 246 \pm 2$ K, for

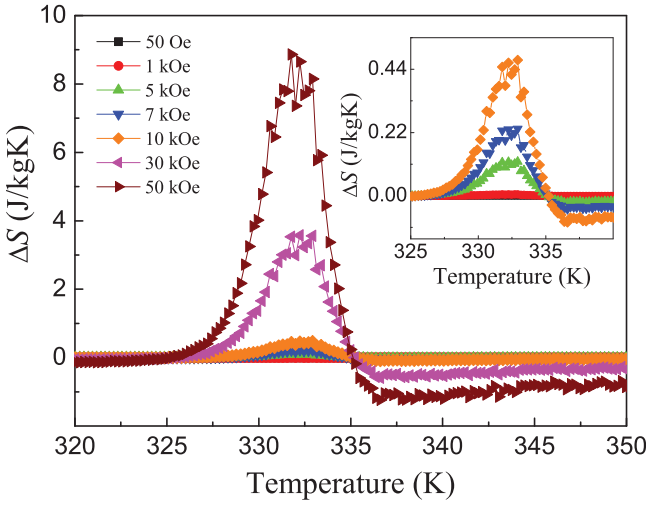

FIG. 5. Magnetic field induced entropy changes as a function of temperature for selected values of the applied field up to 50 kOe. Inset: Detail of the curves corresponding to low applied fields up to 10 kOe.

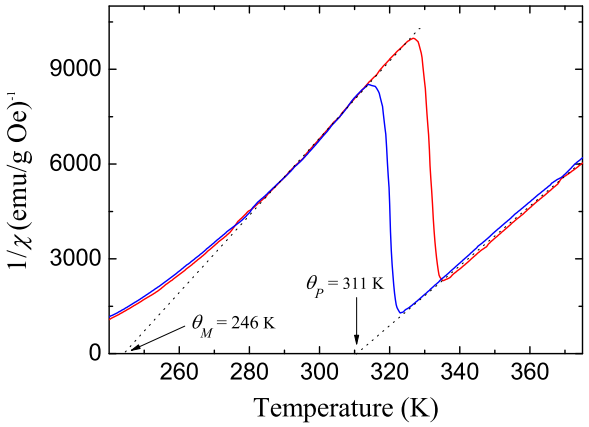

FIG. 6. Inverse of the susceptibility as a function of temperature. Extrapolation to zero of the linear behavior above and below the transition renders the paramagnetic Curie temperatures indicated by arrows.

the martensitic phase. The lower value of the paramagnetic Curie temperature of the martensitic phase is consistent with the occurrence of antiferromagnetic bonds in the martensitic phase. From the slopes, the effective magnetic moments in the parent and martensitic phases can be estimated. We have obtained (per Mn-atom) $\mu_P = 3.61 \pm 0.04 \mu_B$ and $\mu_M = 3.19 \pm 0.04 \mu_B$ (μ_B is the Bohr magneton) which confirms a decrease of the effective magnetic moment at the martensitic transition.

It is interesting to point out that in spite of the paramagnetic character of both parent and martensitic phases, the magnetocaloric effect is considerably large which proves the strong interplay between structure and magnetism in the studied material. We have found that while application of a magnetic field shifts, the martensitic transition to lower temperatures, application of an external stress has the opposite effect. Therefore, an applied magnetic field increases the range of stability of the parent phase, which is reduced by an applied stress. Consequently, the magnetocaloric effect in the vicinity of the martensitic transition is inverse in the studied alloy and the elastocaloric effect is conventional. Another consequence of the opposite effect of a mechanical (stress) and an applied magnetic field on the phase stability of the $Ni_{43}Mn_{40}Sn_{10}Cu_7$ alloy is the fact that the magnetocaloric effect occurs in a single entropy versus temperature peak while two peaks develop in the elastocaloric effect. In both cases, in the range of fields applied in our study, the isothermally induced changes of entropy are modest and significantly lower than the whole available entropy, which, to a good approximation, is given by the difference of entropy between martensitic and parent phases. For instance, the application of a magnetic field of 5 T enables to induce only 15% of the total entropy content. Actually, this is a consequence of the low rate of change of transition temperatures under both applied magnetic fields and stresses. It is worth pointing out that the stresses required in order to induce the whole transition are, in practice, unachievable due to the high brittleness of the studied material.[19]

A meaningful parameter adequate for characterizing the cooling effectiveness of a given material in refrigeration applications is the relative cooling power (*RCP*) defined as[20]

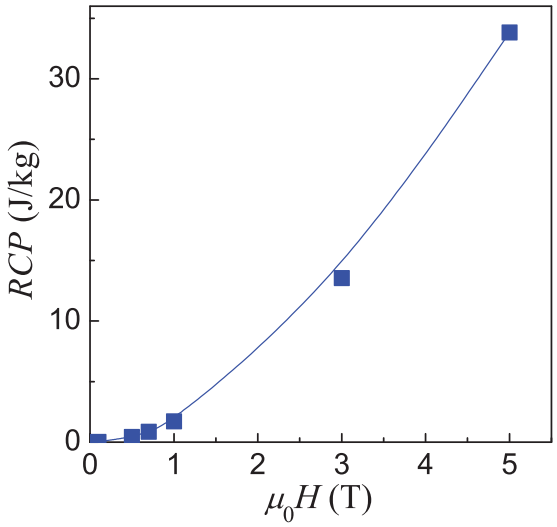

FIG. 7. Magnetic relative cooling power *RCP* as a function of the applied magnetic field, obtained from results shown in Fig. 5.

$$RCP(\sigma, H) = \int_{\Delta T} |\Delta S(T, H, \sigma)| dT, \quad (6)$$

where the range over which the integral is performed, ΔT corresponds to the extension of the peaks giving the field (mechanic or magnetic) induced entropy change. Fig. 7 shows *RCP* in the case of the magnetocaloric effect as function of the applied magnetic field and zero applied stress. It weakly increases for inducing fields below $\mu_0 H < 1$ T, but reasonable values are reached for magnetic field in the range between 2 and 3 T. In the case of the elastocaloric effect, *RCP* has essentially two contributions arising from the two peaks shown in Fig. 3. The *RCP* given in Fig. 8 is the sum of the contributions associated with the two peaks. It is given for selected values of the applied magnetic field. Interestingly, a moderate applied field of 0.7 T enables to increase the relative cooling power by about 40%. Comparing the results for the magnetocaloric and elastocaloric effects, we

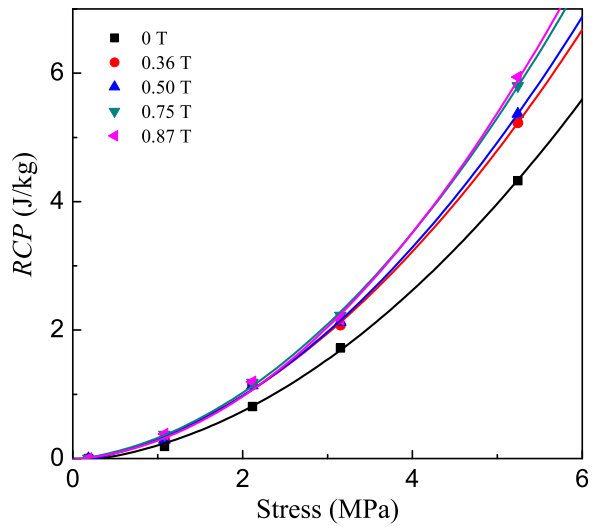

FIG. 8. Elastic relative cooling power *RCP* as a function of the applied stress for selected values of the applied magnetic field obtained from results displayed in Fig. 3.

can conclude that from the point of view of the refrigeration power, application of a magnetic field of about 1.5 T gives similar results than application of a stress of 5 MPa. Finally, it is worth pointing out that the values of the *RCP* obtained in the range from 0 to 6 MPa are comparable to those reported for a NiMnGa(Co) magnetic shape-memory alloy.[15]

In summary, in the present paper we have shown that, thanks to a strong magneto-structural interplay, the combination of elasto- and magnetocaloric effects can considerably improve the refrigeration capacity of a metamagnetic shape-memory alloy that remains paramagnetic in both the parent and martensitic phases. While the obtained values of the *RCP* are still modest in the studied NiMnSn(Cu) alloy, this finding opens interesting perspectives in order design specific devices that take advantage of such combination of multicaloric properties.

ACKNOWLEDGMENTS

This work was supported by CICyT (Spain), project No. MAT-2010-15114 and by CONACYT (México), project CB-157541. Technical support from the *Laboratorio Nacional de Investigaciones en Nanociencias y Nanotecnología*, México, is acknowledged. P.C.-V. acknowledges support from CONACYT (México) under scholarship No. 186474.

[1]K. Ullakko *et al.*, Appl. Phys. Lett. **69**, 1966 (1996).
[2]A. Sozinov, A. A. Likhachev, N. Lanska, and K. Ullakko, Appl. Phys. Lett. **80**, 1746 (2002).
[3]R. Kainuma *et al.*, Nature (London) **439**, 957 (2006).
[4]B. Ingale *et al.*, J. Appl. Phys. **105**, 023903 (2009).
[5]A. Planes, L. Mañosa, and M. Acet, J. Phys. Condens. Matter **21**, 233201 (2009).
[6]T. Krenke, E. Duman, M. Acet, E. F. Wassermann, X. Moya, L. Mañosa, and A. Planes. Nature Mater. **4**, 450 (2005).
[7]S. Aksoy, T. Krenke, M. Acet, E. F. Wassermann, X. Moya, L. Mañosa, and A. Planes, Appl. Phys. Lett. **91**, 241916 (2007).
[8]L. G. de Medeiros, N. A. de Oliveira, and A. Troper, J. Appl. Phys. **103**, 113909 (2008).
[9]L. Mañosa, D. González-Alonso, A. Planes, E. Bonnot, M. Barrio, J. L. Tamarit, S. Aksoy, and M. Acet, Nature Mater. **9**, 478 (2010).
[10]L. Mañosa, D. González-Alonso, A. Planes, M. Barrio, J. L. Tamarit, I. S. Titov, M. Acet, A. Bhattacharya, and S. Majumdar, Nature Comm. **2**, 595 (2011).
[11]E. Bonnot, R. Romero, L. Mañosa, E. Vives, and A. Planes, Phys. Rev. Lett. **100**, 125901 (2008).
[12]D. E. Soto-Parra, E. Vives, D. González-Alonso, L. Mañosa, A. Planes, R. Romero, J. A. Matutes-Aquino, R. A. Ochoa-Gamboa, and H. Flores-Zúñiga, Appl. Phys. Lett. **96**, 071912 (2010).
[13]D. H. Wang, C. L. Zhang, H. C. Xuan, Z. D. Han, J. R. Zhang, S. L. Tang, B. X. Gu, and Y. W. Du, J. Appl. Phys. **102**, 013909 (2007).
[14]R. Das, S. Sarma, A. Perumal, and A. Srinivasan, J. Appl. Phys. **109**, 07A901 (2011).
[15]P. O. Castillo-Villa, D. E. Soto-Parra, J. A. Matutes-Aquino, R. A. Ochoa-Gamboa, D. González-Alonso, L. Mañosa, A. Planes, R. Romero, M. Stipcich, H. Flores Zúñiga, and D. Ríos-Jara, Phys. Rev. B **83**, 174109 (2011).
[16]S. Aksoy, M. Acet, P. P. Deen, L. Mañosa, and A. Planes, Phys. Rev. B **79**, 212401 (2009).
[17]V. D. Buchelnikov, P. Entel, S. V. Taskaev, V. V. Sokolovskiy, A. Hucht, M. Ogura, H. Akai, M. E. Gruner, and S. K. Nakay, Phys. Rev. B **78**, 184427 (2008).
[18]V. V. Sokolovskiy, V. D. Buchelnikov, M. A. Zagrebin, P. Entel, S. Sahool, and M. Ogura, Phys. Rev. B **86**, 134418 (2012).
[19]J. Pons, E. Cesari, C. Seguí, F. Masdeu, and R. Santamarta, Mater. Sci. Eng. A **481-482**, 57 (2008).
[20]K. A. Gschneidner, V. K. Pecharsky, and A. O. Tsokol, Rep. Prog. Phys. **68**, 1479 (2005).